



## PHYTONUTRIENT ASSISTED SYNTHESIS AND STABILIZATION OF SILVER NANOPARTICLES FROM THE ROOT EXTRACT OF *MIRABILIS JALAPA* AND THEIR ANTIBACTERIAL ACTIVITY STUDIES

M. P. Somashekarappa\*, H. B. Nandeesh

Department of PG Studies in Chemistry, IDSG College, Chikkamagaluru, Affiliated to Kuvempu University, Karnataka State, India

\*Corresponding author: [mpsomashekar1@gmail.com](mailto:mpsomashekar1@gmail.com)

Received: 22-12-2022; Accepted: 04-02-2023; Published: 28-02-2023

© Creative Commons Attribution-NonCommercial-NoDerivatives 4.0 International License <https://doi.org/10.55218/JASR.202314207>

### ABSTRACT

Silver nanoparticles (AgNPs) were synthesized using the aqueous root extract of a medicinal plant, *Mirabilis jalapa*. The particles were characterized using UV-visible spectroscopy, scanning electron microscopy (SEM), transmission electron microscopy (TEM) and powder X-ray diffraction (PXRD) studies. The average particle size of the AgNPs worked out using PXRD and TEM results are 13-15 nm. Silver in the nanoparticles is found to crystallize in to face centred cubic structure. Effect of the nanoparticles against the growth of *Escherichia coli* (*E. coli*) and *Staphylococcus aureus* (*S. aureus*) bacteria were determined. The AgNPs inhibit the spread of both the bacteria, but to different extents and the minimum inhibitory concentration of the AgNP solution is  $29.0 \times 10^{-5}$  g/mL against *E. coli*, and  $25.4 \times 10^{-5}$  g/mL against *S. aureus*.

**Keywords:** Antibacterial activity, *Escherichia coli*, *Mirabilis jalapa*, Silver nanoparticles, *Staphylococcus aureus*.

### 1. INTRODUCTION

Silver nanoparticles (AgNPs) are an extensively explored class of metallic nanomaterials, for enormous industrial applications, owing to their size-dependant physico-chemical properties [1]. Performance characteristics of any devices fabricated from the nanomaterials depends on the size, shape, structure of individual particle units, and the mechanical stability of the fabricated devices. Surface Plasmon resonance is understood to be the main size, shape and structure dependant physico-chemical property that makes AgNPs applicable in various fields [2]. The diverse areas of the applications of the AgNPs encompasses photocatalysis [3], optical sensors [4], nanosphere lithography [5], optoelectronics [6], solar energy conversion devices [7] and surface-enhanced Raman scattering (SERS) substrates [8]. In addition, AgNPs are very much known for their antimicrobial activities [9] leading to various biomedical applications. Representative and selective reviews pertaining to biomedical applications are referenced here [10-12]. The potential industrial applications led by antimicrobial properties of the AgNPs include AgNP embedded polyurethane based

antibacterial water filter [13], AgNP impregnated blotting paper based point-to-use antibacterial water filter [14, 15], AgNP embedded activated carbon based antibacterial air filter [16] and AgNP embedded textile fabrics possessing antibacterial properties [17-20]. Recent evolution of AgNPs in theranostics has been reviewed [21].

Using various traditional chemical reducing agents such as  $\text{NaBH}_4$ ,  $\text{LiAlH}_4$ ,  $\text{R}_4\text{N}^+(\text{Et}_3\text{BH}^-)$  or hydrazine [22], for the synthesis of AgNPs results in unstable particle solutions containing reaction by-products such as borides, metal borates [23],  $\text{B}_2\text{H}_6$ ,  $\text{NaNO}_3$  etc. The traditional reduction methods also demands use of various stabilizing agents [24], certain polymers, and cationic polynorbornenes [25], making the synthesis and stabilization of AgNPs expensive harmful and multistep one's. The synthesis of AgNPs by using mixed-valence polyoxometallates, polysaccharide, Tollens irradiation and biological methods have been regarded as greener approaches [26]. However, synthesis of AgNPs using extracts of plants, bacteria, fungi and biopolymers are greener and cheaper method in recent years [27-29]. It has also been established that the sensitivity of AgNPs

synthesized from plant extracts, for biosensing of fungicide and photocatalytic properties are relatively better [30].

*Mirabilis jalapa* is used extensively as a medicinal plant in almost all folklore remedies around the world for treating various diseases as the extracts of this plant shows antibacterial, antiviral and antioxidant activities [31, 32]. Chemical analysis of various parts of *Mirabilis jalapa* revealed the presence of alkaloids, flavonoids, phenols, steroids, triterpenes, glycosides, tannins, saponins and lignins. The extracts of this plants are analysed to have alanine, arabinose, campesterol, daucosterol and dopamine, d-glucan, hexacon-1-ol, indicaxanthin, isobetanin, 6-methoxyboeravinone, C-methylabronisoflavones, miraxanthins, n-dotriacontane, n-nonacosane, n-pentacosane, n-triacontane. Extracts of *Mirabilis jalapa* are proved to exhibit a wide variety of pharmacological and therapeutic effects as antimicrobial, antiparasitic, dermatological, anticancer, anti-inflammatory, analgesic, anti diabetic, antihistaminic, immune-modulatory, antispasmodic [33, 34]. Seeds of *Mirabilis jalapa* contains  $\beta$ -sitosterol,  $\beta$ -amyrin and  $\beta$ -sitosterol-D-glucoside [35]. Though, silver nanoparticles were synthesized from the leaf extract of *Mirabilis jalapa* complete characterization is not been realized [36]. However, synthesis of AgNPs from the aqueous root extract of *Mirabilis jalapa* has not been reported. Therefore in this report we describe the synthesis of AgNPs from the root extract of *Mirabilis jalapa*, their complete characterization by Uv-visible extinction spectroscopy, powder X-ray diffraction, SEM and TEM analysis, and the study of their antibacterial activities against *E. coli* and *S. aureus* bacteria.

## 2. MATERIAL AND METHODS

### 2.1. Materials

The nutrient agar media is from Himedia. The chemicals were from Merck, or from S. D. Fine chemicals. Distilled water was used wherever required. Bacteria selected for the study were *E. coli* and *S. aureus*. A laboratory centrifuge, R-8C from Remi was used for isolation of particles for SEM and powder XRD analyses. Systronics Uv-visible spectrophotometer 119 was used for recording the Uv-visible extinction spectra in the wavelength range of 300 nm to 700 nm. Powder XRD patterns were recorded on a Rigaku Smartlab X-Ray diffractometer and the SEM and EDS were recorded on Ultra 55 scanning electron microscope from GEMINI technology. TEM imaging of the drop

coated samples were done on Titan Themis 300kV from FEI.

### 2.2. Methods

#### 2.2.1. Extraction

Freshly harvested root of the plant were sliced, crushed in to paste with a little amount of warm distilled water using mortar and pestle. The paste was transferred in to a 250 mL beaker, suspended in 100 mL water, stirred on a magnetic stirrer for about 30 minutes at 45-50°C temperature, cooled to lab temperature and filtered through a pre-weighed piece of qualitative filter paper. The weight of the contents transferred to the extract was calculated by difference in weight method. Qualitative phytochemical analysis of the extract was done following routine methods [37].

#### 2.2.2. Synthesis of Silver Nanoparticles

A 50 ml of the fresh extract containing approximately  $0.04 \pm 0.005$  g/mL of extracted substances was taken in a round bottomed flask fitted with a pressure equalizing dropping funnel. It was heated to 60°C while stirring and 20mL of 0.002 M AgNO<sub>3</sub> solution was added drop wise. Temperature was maintained at  $60 \pm 5^\circ\text{C}$  during addition of AgNO<sub>3</sub> solution and for further 1 hour's time. Contents were cooled to lab temperature. AgNP solution so obtained was centrifuged for isolation of the material, for powder XRD and SEM analyses. The solid was then dried in vacuum over anhydrous phosphorous pentoxide and powdered.

#### 2.2.3. Antibacterial Activity Studies

A known volume of the AgNP solution was evaporated on a pre weighed watch glass, dried and weighed to determine the amount of AgNP material in its solution. A suspension 28 grams of nutrient agar in 1000 mL of distilled water was boiled and autoclaved. 20 mL aliquots of the nutrient agar media were contaminated with various increased concentration of AgNP solutions and transferred in to sterilized Petri dishes. When the media hardened, surface of the media were applied with stains of selected bacteria using cotton swabs. The growth or spread of bacteria was followed for a period of 12 to 15 hours. The standard reference for analysis of the data was the results of same experiments using ciprofloxacin conducted at same condition.

## 3. RESULTS AND DISCUSSION

Water extracts of the root sample of the selected plant with a total phytonutrient concentration of  $20 \times 10^{-3}$

g/mL, was subjected to qualitative phytochemical analyses using routine procedures [37]. Presence of alkaloids, carbohydrates and glycosides, saponines, and phenolic acids and flavonoids were confirmed reproducibly and the results are consistent with the reported literature [31].

In order to be applicable in biology and medicine stability of the AgNPs in all sizes and their biocompatibility is an important requirement [26]. AgNPs synthesized using relatively harsh reducing agents such as sodium borohydride and without any stabilizing agents are unstable. It is expected that, presence of phytonutrient molecules with flavones and triterpenoid structures, render the extract with free radical scavenging ability [31], which in turn is of reducing nature. Thus addition of silver salt in to the extract results in formation of metallic silver particles in nano dimensions.

### 3.1. Synthesis

The extract solution used for synthesis of AgNPs contained approximately  $8 \times 10^{-4}$  g/mL of phytonutrients. The AgNPs synthesized using root extract of

*Mirabilis jalapa* and without any reducing agents and stabilizing agents are very much stable and the procedure is highly reproducible. The drop wise addition of the  $\text{AgNO}_3$  solution in to an extract containing the phytochemical molecules belonging to phenolic compounds and flavonoids, analysed as a part of this work and reported in earlier precedent [31] reduces the  $\text{Ag}^+$  in the  $\text{AgNO}_3$  in to atomic silver [28, 38-40] that condenses in to particles of nanometer dimensions. The particles so condensed in the medium of extract are then coated with various bioactive molecules available in the solution to form a protective monomolecular layer [30, 41]. Particles coated with same kind of organic layer throughout the dispersion medium possess same charge and hence repel with each other. Thus the AgNPs synthesized by this method are highly stable.

### 3.2. Characterization

Fig.1 shows the uv-visible extinction spectrum of the AgNPs synthesized using water extract of root of *Mirabilis jalapa*.

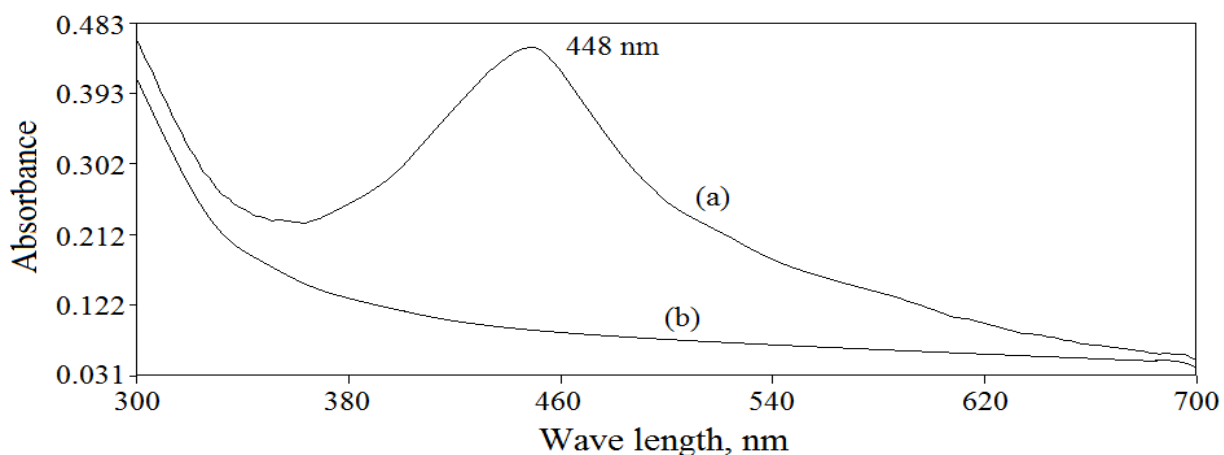


**Fig. 1: (a) Uv-visible extinction spectrum of the AgNPs synthesized from the extract of *Mirabilis jalapa* (b) Uv-visible absorption spectrum of the extract before formation of AgNPs**

A characteristic surface plasmon resonance absorption band due to surface electrons, in the uv-visible region of electromagnetic radiation is indication of the presence of silver nanoparticles [42, 43]. In addition to a qualitative visual indication of change in colour of the extract from colourless to reddish brown upon addition of  $\text{AgNO}_3$ , formation of AgNPs could be confirmed by recording a Uv-visible absorption spectrum in the region of 300-700 nm [44, 45]. Fig. 1(a) shows the Uv-

visible spectrum recorded for the AgNPs obtained from the reaction between extract of *Mirabilis jalapa* and  $\text{AgNO}_3$  solution and the data is consistent with the Uv-visible absorption characteristics of the AgNPs synthesized by reduction of silver nitrate with hydrazine hydrate and sodium citrate [46]. The spectrum recorded for the extract before addition of silver nitrate in the same wavelength range results in only a baseline without any absorption peak (fig. 1(b)). The  $\lambda_{\text{max}}$  is observed at

448 nm, and a bigger full width at half maximum (FWHM) of the peak appear to be consisted of many number of overlapping extinction bands indicating a relatively wider distribution of particle size. Upon repeated recording of the spectrum for the same AgNP solution with a regular interval of two weeks, and for period of 60 days, the intensity of the absorption peak did not decrease. This observation indicates that the particles are highly stable in the dispersion medium.

The synthesized AgNPs were isolated by centrifugation at 4000 rpm and the SEM and EDS studies were done on the powder samples in order to understand morphology and elemental composition of silver and other elements in the material. Fig. 2 shows the SEM image of the AgNPs synthesized from the root extract of *Mirabilis jalapa*.

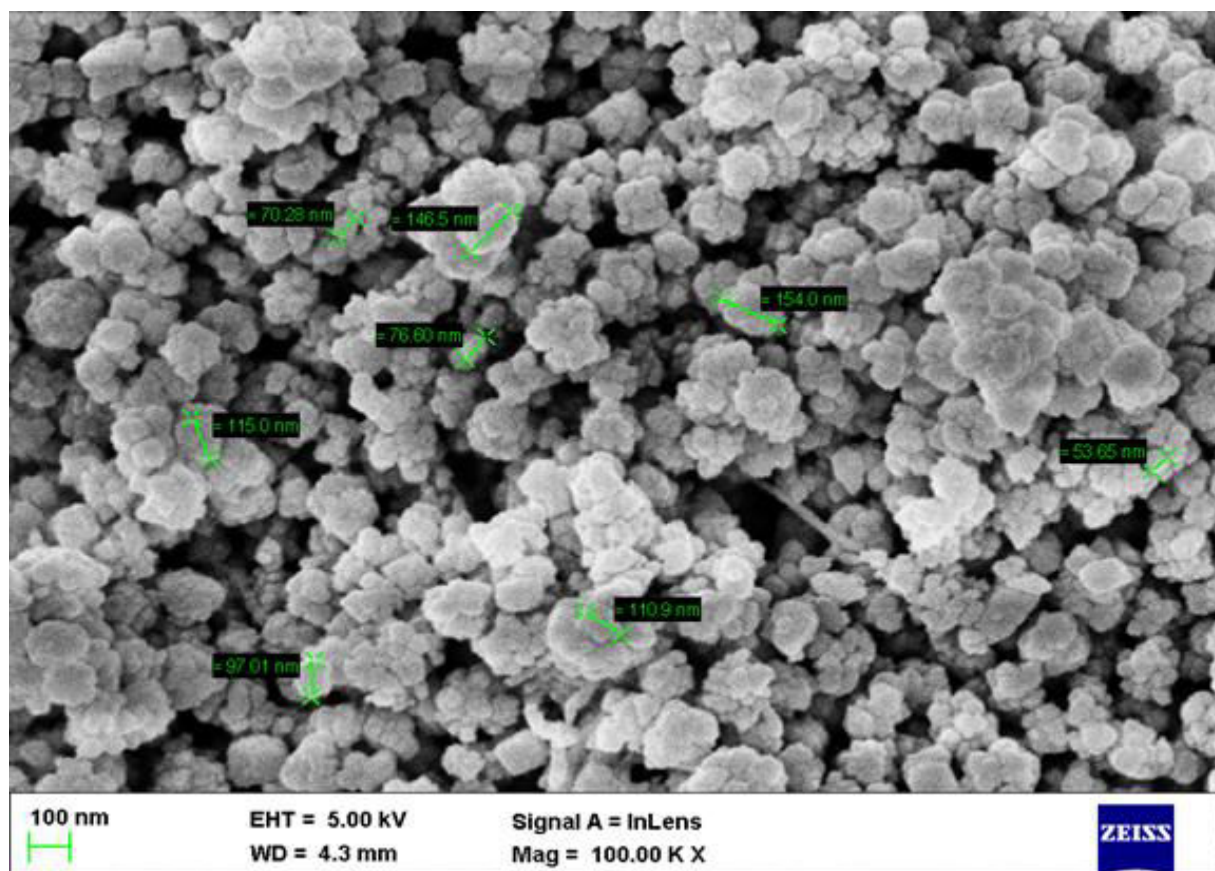


**Fig. 2: Scanning electron micrograph of AgNPs synthesized from the root extracts of *Mirabilis jalapa***

It is clear from the SEM image of the isolated material that the AgNPs synthesized are spherical and coalesced to form bigger aggregates of sizes ranging from  $\sim 54$  nm to  $\sim 154$  nm. These spherical agglomerates must have been formed during centrifugation. The point EDS analysis done in order to profile the elements present, on the micron sized aggregates (fig. 3(a)) of the AgNPs material indicates the presence of 65.23% by weight of Ag, 6.82% C, 11.46 % N and 16.50 % O (inset in fig. 3 (b)). Presence of oxygen, nitrogen and carbon in the EDS analysis may be ascribed to the involvement of monomolecular layer of phytonutrient molecules on the particles and hence stabilizing them.

The AgNPs obtained by the present method appear spherical and quasi spherical with a higher percentage of spherical particles (Fig. 4). All the particles less than 20 nm are spherical.

Our TEM results are in good agreement with results of earlier researchers. Some selective earlier precedents are mentioned here. Synthesis of AgNPs from the plant extract of *Terminalia bellirica* results in spherical particles [47], and the AgNPs obtained by extracellular synthesis using Fungus, *Aspergillus niger* are also spherical [48]. Quasispherical shaped particles of AgNPs were synthesized using apiin as reducing agent [49]. The particle size distribution worked upon the TEM image

given in figure 4 reveals that the maximum particle size passes through 13-20 nm (inset in fig. 4). It is clear from comparison of SEM and TEM images that the particle aggregates of size ranging from  $\sim 54$  nm to  $\sim 154$  nm appeared in SEM image must have been formed due to agglomeration of the particles into bigger aggregates

during centrifugation and drying in vacuum, and due to the presence of organic matter in the form of protective layer on the particles. Fig.5 (a) shows a HRTEM image of a single spherical silver nanoparticle whose size is 20 nm.

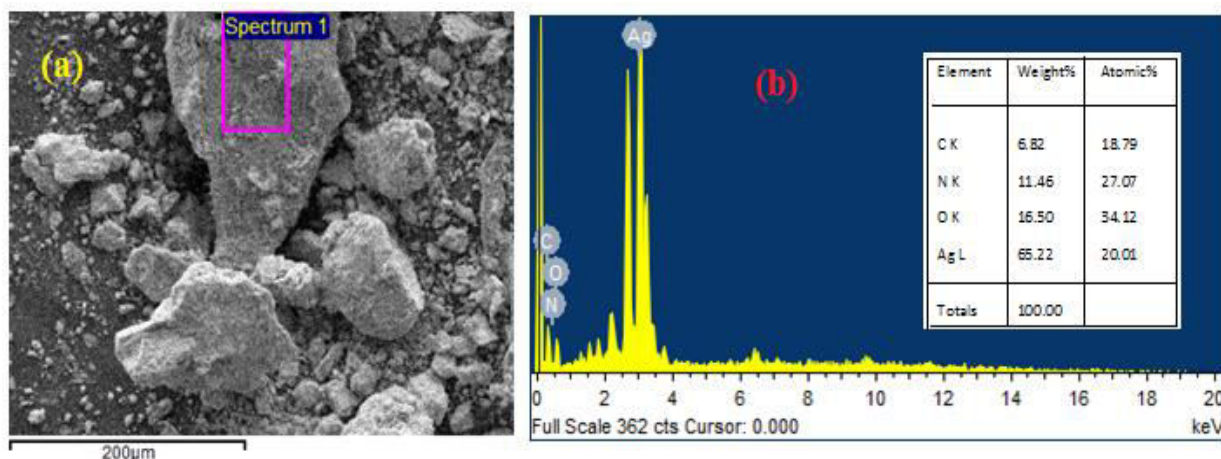
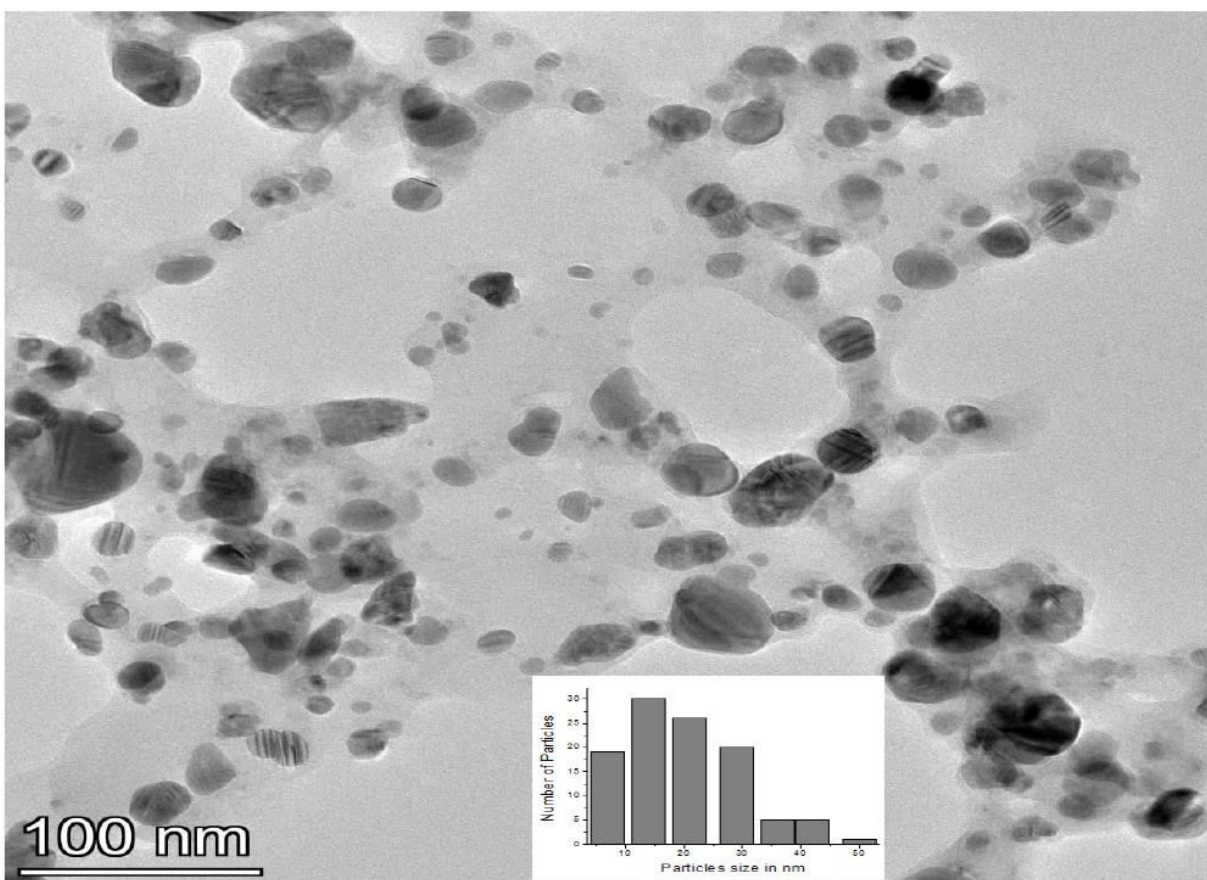
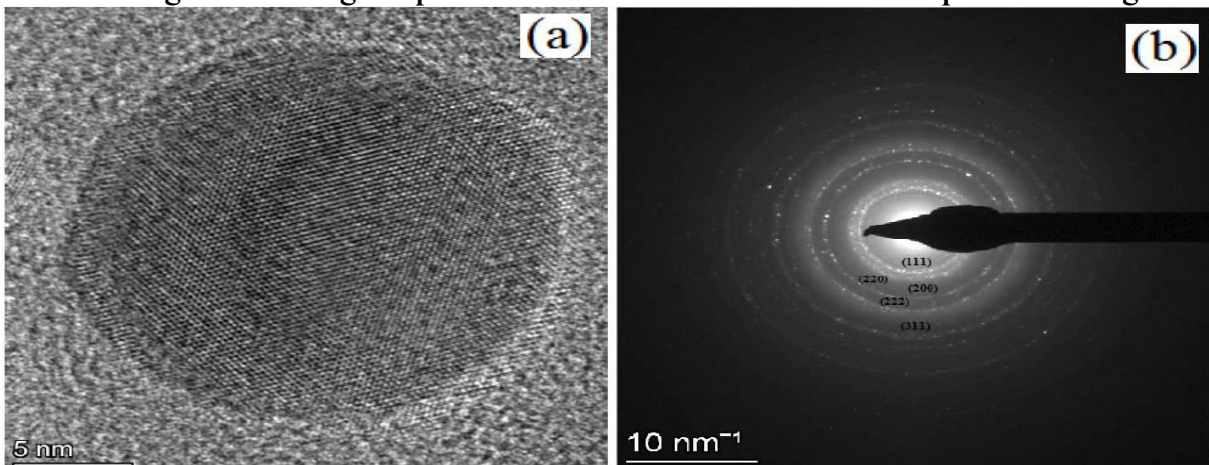


Fig. 3: (a) Micron sized material aggregates upon which the point EDS was recorded and (b) the EDS spectrum of the silver nanoparticles synthesized using the extract of *Mirabilis jalapa*. Inset in (b) Table showing the elemental percentage of silver, carbon, nitrogen and oxygen in the material



**Fig. 4: Transmission electron micrographs of the AgNPs synthesized from the extracts of *Mirabilis jalapa*. Inset: Histogram showing the particle size distribution worked out upon TEM image**



**Fig. 5: (a) High resolution TEM image of the single 20 nm sized silver nanoparticle synthesized from the root extract of *Mirabilis jalapa*. (b) SAED pattern on the drop casted layer of AgNP solution**

Selected area electron diffraction (SAED) pattern recorded on a thin layer of AgNPs drop casted from its solution exhibits concentric circles embedded with bright intermittent dots (fig. 5(b)). Radii of these concentric circles represents diffraction from 111, 200, 220, 222 and 311 planes of face centered cubic (FCC) structure of crystalline AgNPs. This confirms that the reduction of silver nitrate by the phytonutrient molecules in the root extract of *Mirabilis jalapa* results in crystallization of the silver atoms in to a FCC structure in their nanoparticles [46]. This result of our work is in fair agreement with that of AgNPs synthesized both by chemical reduction method and by using extract of *Hibiscus rosasinensis* [50].

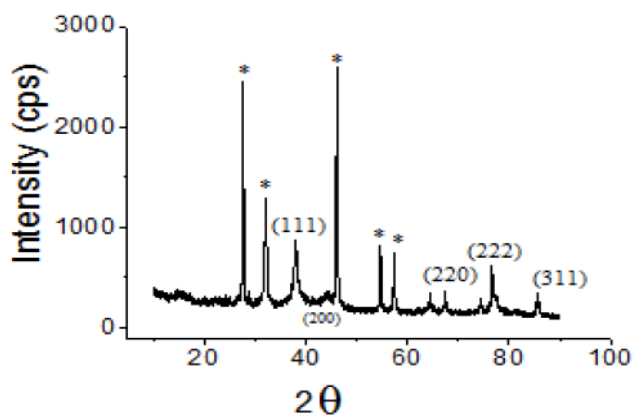


**Fig. 6: Powder XRD pattern of AgNPs synthesized from the root extract of *Mirabilis jalapa***

AgNPs material in the powder form was obtained by centrifugation of their solution and the powder XRD pattern was recorded in order to understand averaged out particle size and crystal structure. PXRD pattern is shown in fig. 6.

The positions of the crystallographic planes (111), (200), (220), (222) and (311) in the Powder XRD pattern recorded upon the powder sample are indicative of silver in the silver nitrate being reduced by phytonutrient molecules and crystallized in to face centered cubic (FCC) structure. Relatively bigger FWHM of the peaks in the PXRD pattern shows that the material is in the form of nanocrystallites. The average particle size corresponding to (111) crystallographic plane was calculated using Debye - Scherrer's formula  $D = 0.94 \lambda / \beta \cos \theta$ , where D is the average crystalline size,  $\lambda$  is the wavelength of X-ray,  $\beta$  is FWHM  $\theta$  is the angle of diffraction. Average particle size of the AgNPs synthesized using the root extract of *Mirabilis jalapa* is worked out to be 15 nm. This value of particle size is consistent with the particle size distribution obtained by TEM analysis. The PXRD peaks corresponding to various crystallographic planes obtained for the AgNPs synthesized from root extract of *Mirabilis jalapa* are comparable and consistent those obtained for AgNPs synthesized using aqueous extract of *Ocimum Sanctum* and quercetin (a flavonoid from the same plant) [51], root hair extract of *Phoenix dactylifera* [52], extracts of garlic, green tea and turmeric [53], extract of *Sida cordifolia* [54]. The other sharp PXRD signals, indicated by asterisk in figure 6 may be due to

crystallization of other phytonutrient molecules which are not involved either in reduction of  $\text{AgNO}_3$  or capping of the particles, on the surface of the particles or particle aggregates.

### 3.3. Antimicrobial activity studies

Inhibitory effects of the AgNPs against the growth of *E. coli* and *S. aureus* bacteria are presented in fig. 7 and fig. 8 respectively.

Silver nanoparticles are very much known for their characteristic antimicrobial activity [55]. Elaborate reviews of the studies related to antimicrobial activities of the AgNPs synthesized by various methods were preceded in literature [56, 57]. We consider in this study, the relative assessment of antibacterial property of the title AgNPs, with respect a reference substance, as a representative application. An increase in concentration of the AgNPs in the solidified solution of nutrient agar media decreases the growth of bacteria.

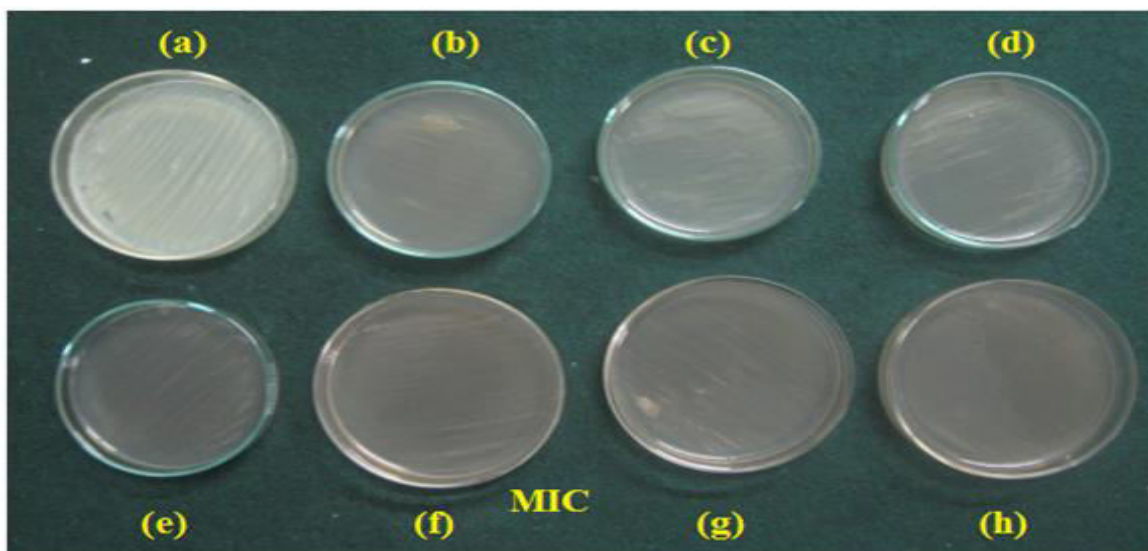


Fig. 7: Growth of the *E. coli* bacteria in 20 ml nutrient agar media contaminated with (a) 0.00 g/ml, (b)  $1.45 \times 10^{-4}$  g/mL, (c)  $1.4125 \times 10^{-4}$  g/mL, (d)  $2.175 \times 10^{-4}$  g/mL (e)  $2.5375 \times 10^{-4}$  g/mL, (f)  $2.90 \times 10^{-4}$  g/mL (g)  $3.2625 \times 10^{-4}$  g/mL, (h)  $3.625 \times 10^{-4}$  g/mL of silver nanoparticles prepared from extract of *Mirabilis jalapa*

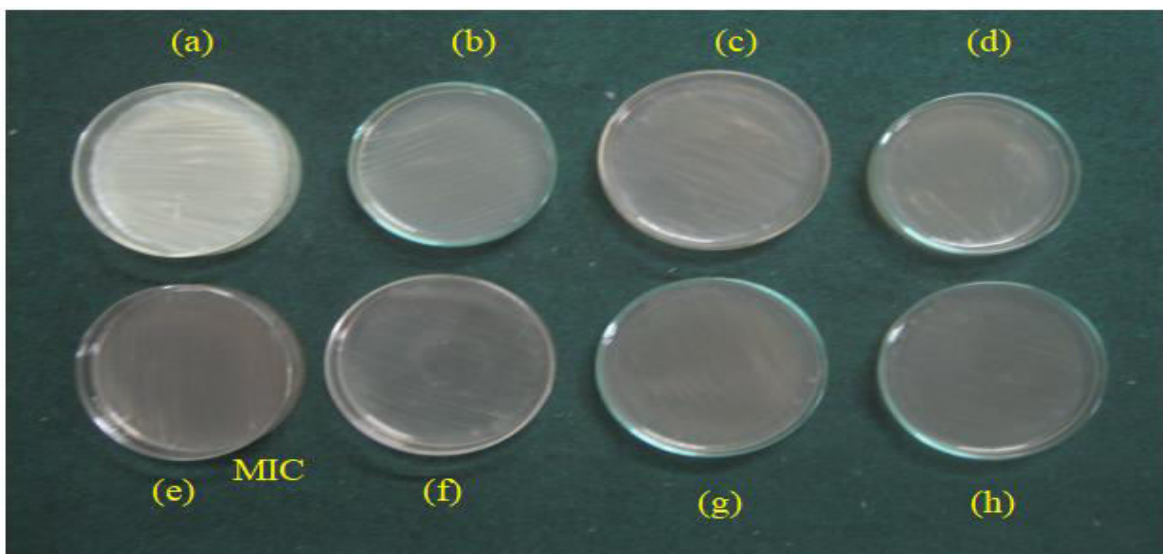


Fig. 8: Growth of the *S. aureus* bacteria in 20 ml nutrient agar media contaminated with (a) 0.00 g/ml, (b)  $1.45 \times 10^{-4}$  g/mL, (c)  $1.4125 \times 10^{-4}$  g/mL, (d)  $2.175 \times 10^{-4}$  g/mL (e)  $2.5375 \times 10^{-4}$  g/mL, (f)  $2.90 \times 10^{-4}$  g/mL (g)  $3.2625 \times 10^{-4}$  g/mL, (h)  $3.625 \times 10^{-4}$  g/mL of silver nanoparticles prepared from extract of *Mirabilis jalapa*

A minimum possible concentration of AgNPs in the media above which bacteria cannot spread is known as minimum inhibitory concentration (MIC). The determined MIC of the silver nanoparticles prepared from the root extract of *Mirabilis jalapa* against the spreading of *E. coli* bacteria is  $29.00 \times 10^{-5}$  g/mL (figure 7) and it is  $25.37 \times 10^{-5}$  g/mL (figure 8) against the growth of *S. aureus*, in the experimental conditions maintained. The experimentally determined MIC of the ciprofloxacin is  $20 \times 10^{-5}$  g/mL against *E. coli* and  $24 \times 10^{-5}$  g/mL against the spread of *S. aureus* bacteria respectively in the same experimental conditions.

#### 4. CONCLUSION

A dilute aqueous extract of the medicinal plant *Mirabilis jalpa*, containing phytonutrients such as alkaloids, carbohydrates, glycosides, saponines, phenolic acids and flavonoids, acts as both reducing and stabilizing medium for the synthesis of silver nanoparticles. The size of silver nanoparticles obtained is evaluated to be 13-15 nm using PXRD and TEM techniques. The crystallographic planes in PXRD pattern and the concentric rings in SAED spectrum are indicative of silver being crystallized in to FCC structure in their spherical and quasi-spherical nanosized particles. The MICs of AgNPs synthesized from the root extract of *Mirabilis jalapa* against the spread of *E. coli* and *S. aureus* bacteria were found to be  $29.00 \times 10^{-5}$  g/mL and  $25.37 \times 10^{-5}$  g/mL respectively.

#### 5. ACKNOWLEDGEMENTS

Authors thank VGST for awarding a K-FIST level-1 grant which was used to establish basic laboratory facility. Author also thank Micro and Nano characterization facility, Center for nanoscience and engineering, IISc., Bangalore for extending characterization support under INUP programme. Authors also thank Dr. B. Thippeswamy, department of Microbiology, Kuvempu University for giving bacteria. This research did not receive any specific grant from funding agencies in the public, commercial, or not-for-profit sectors.

#### Conflict of interest

Authors declare that they have no conflicts of interest.

#### 6. REFERENCES

1. Stark WJ, Stoessel PR, Wohlleben W, Haffner A. *Chem Soc Rev*, 2015; **44**:5793-5905.
2. Amendola V, Bakr OM, Stellacci F. *Plasmonics*, 2010; **5**:85-97.
3. Awazu K, Fujimaki M, Rockstuhl C, Tominaga J, Murakami H, Ohki Y, et al. *J Am Chem Soc*, 2008; **130(5)**:1676-1680.
4. McFarland AD, Van Duyne RP. *Nano Lett*, 2003; **3**:1057-1062.
5. Jensen TR, Malinsky MD, Haynes CL, Van. Duyne RP. *J Phys Chem B*, 2000; **104**:10549-10556.
6. Ko S-J, Choi H, Lee W, Kim T, Lee BR, Jung J-W, et al. *Energ Environ Sci*, 2013; **6**:1949-1955.
7. Morfa AJ, Rowlen KL. *Appl Phys Lett*, 2008; **92**:013504.
8. Li W, Guo Y, Zhang P, *J Phys Chem C*, 2010; **114**:6413-6417.
9. Rai M, Yadav A, Gade A. *Biotechnol Adv*, 2009; **27**:76-83.
10. Wong KKY, Liu X. *Med Chem Commun*, 2010; **1**:125-131.
11. Prabhu S, Poulouse EK. *Int Nano Lett*, 2012; **2**:32.
12. Burdusel AC, Gherasim O, Grumezescu AM, Mogoanta L, Ficai A, Andronescu E. *Nanomaterials*, 2018; **8(9)**:681.
13. Jain P, Pradeep T. *Biotechnol Bioeng*, 2005; **90**:59.
14. Dankovick TA, Gray DG. *Environ Sci Technol*, 2011; **45**:1992-1998.
15. Praveena SM, Karuppaiah K, Than LTL. *Cellulose*, 2018; **25**:2647-2658.
16. Yoon KY, Byeon JH, Park CW, Hwang J. *Environ Sci Technol*, 2008; **42**:1251-1255.
17. Ravindra S, Mohan YM, Reddy NN, Raju KM. *Colloids Surf A: Physicochem Eng Asp*, 2010; **367**:31-40.
18. Song J, Kang H, Lee C, Hwang SH, Jang J. *ACS Appl Mater Interfaces*, 2012; **4**:460-465.
19. Wu M, Ma B, Pan T, Chen S, Sun J. *Adv Functional Mater*, 2016; **26(4)**:569-576.
20. Zhang S, Tang Y. Vlahovic B, *Nanoscale Res Lett*, 2016; **11**:80.
21. Shaki Devi R, Girigoswami A, Siddarth M, Girigoswami K. *Appl Biochem Biotechnol*, 2022; **194**:4186-4219.
22. Schmid G, Chi LF. *Adv Mater*, 1998; **10**:515-526.
23. Glavee GN, Klabunde KJ, Sorensen CM, Hadjapanayis. *Langmuir*, 1992; **8**:771-773.
24. Garcia-Barrasa J, López-de-Luzuriaga JM, Monge M. *Cent Eur J Chem*, 2011; **9**:7-19.
25. Baruah B, Gabriel GJ, Akbashey MJ, Booher ME. *Langmuir*, 2013; **29**:4225-4234.
26. Sharma VK, Yngard RA, Lin Y. *Adv Colloid and Interface Sci*, 2008; **145**:83-96.

27. Mittal AK, Chisti Y, Banerjee UC. *Biotechnol Adv*, 2013; **31**:346-356.
28. Rajeshkumar S, Bharath LV. *Chem - Biol Interactions*, 2017; **273**:219 -227.
29. Tarannum M, Divya, Gautam YK. *RSC Adv*, 2019; **9**:34926-34948.
30. Alex KV, Pavai PT, Rugmini R, Shiva Prasad M, Kamakshi K, Chandrashekar K. *ACS Omega*, 2020; **5(22)**:13123-13129.
31. Gogoi J, Nakhura KS, Policegoudra RS, Chattopadhyay P, Rai AK, Veer V. *J Tradit Compliment Med*, 2016; **6**:41-47.
32. Sathish kumar BY, Fathima E. *J Pharmacog Phytochem*, 2017; **6(6)**:1502-1508.
33. Saha S, Deb J, Deb NK. *Int J Herb Med*, 2020; **8(2)**:14-18.
34. Al- Snafi AE, Taleb TA, Jabbar WM, Alqahtani AM. *Int J Biol Pharm Sci Arch*, 2021; **1(2)**:034-045.
35. Singh M, Akash, Mittal SK, Kalia AN. *Int J Pharm Med Appl Sci*, 2012; **1(3)**:22-43.
36. Asha S, Thirunavukkarasu P, Rajeshkumar S. *Res J Pharm Technol*, 2017; **10(3)**:811-817.
37. Raaman N. *Phytochemical Techniques*, New India, Publishing Agency, New Delhi, 2006.
38. Mandal D, Kumar Dash S, Das B, Chattopadhyay S, Ghosh T, Das D, et al. *Biomed. Pharmacother*, 2016; **83**:548-558.
39. Priya RS, Geetha D, Ramesh PS. *Ecotoxicol Environ Saf*, 2016; **134**:308-318.
40. Gopinath K, Kumaraguru S, Bhakyaraj K, Mohan S, Venkatesh KS, Esakkirajan M, et al. *Microb Pathog*, 2016; **101**:1-11.
41. Garcia-Barrasa J, López-de-Luzuriaga JM, Monge M. *Cent Eur J Chem*, 2011; **9**:7-19.
42. Taleb A, Petit C, Pileni MP. *J Phys Chem B*, 1998; **102**:2214-2220.
43. Nogin ov MA, Zhu G, Bahoura M, Adegoke J, Small CE, Ritzo BA, et al. *Opt Lett*, 2006; **31(20)**: 3022-3024.
44. Paramelle D, Sadovoy A, Gorelik S, Free P, Hogley J, Fernig DH. *Analyst*, 2014; **139(19)**:4855-4861.
45. Desai R, Mankad V, Gupta SK, Jha PK. *Nanosci Nanotechnol Lett*, 2012; **4**:30-34.
46. Guzman MG, Dille J, Godet S. *Int J Chem Biomol Eng*, 2009; **2**:104-111.
47. Anand KKH, Mandal BK. *Spectrochim Acta A Mol Biomol Spectrosc*, 2015; **135**:639-645.
48. Gade AK, Bonde P, Ingle AP, Marcato PD, Duran N, Rai MK. *J Biobased Mater Bioenergy*, 2008; **2(3)**: 243-247.
49. Kasturi J, Veerapandian S, Rajendran N, *Colloids and Surfaces B: Biointerfaces*, 2009; **68(1)**:55-60.
50. Philip D. *Physica E: Low Dimens Sys. Nanostruct*, 2010; **42**:1417-1424.
51. Jain S, Mehata, MS, *Scientific Reports*, 2017; **7**: Article 15867.
52. Oves M, Aslam M, Rauf MA, Qayyum S, Qari HA, Khan MS, et al. *Mater Sci Eng C*, 2018; **89**:429-443.
53. Selvan DA, Mahendran D, Senthil Kumar R, Rahiman AK. *J Photochem Photobiol B: Biol*, 2018; **180**:243 - 252.
54. Pallela PNVK, Ummey S, Ruddaraju LK, Pammi SVN, Yoon S-G. *Microb Pathog*, 2018; **124**:63-69.
55. Xiu ZM, Zhang QB, Puppala HL, Colvin VL, Alvarez PJJ. *Nano Lett*, 2012; **12(8)**:4271-4275.
56. Le Ouay B, Stellacci F. *Nanotoday*, 2015; **10(3)**: 339-354.
57. Roy A, Bulut O, Some S, Mandal AK, Yilmaz MD. *RSC Adv*, 2019; **9**:2673-2702.